

# UniTraj: Learning a Universal Trajectory Foundation Model from Billion-Scale Worldwide Traces

Yuanshao Zhu<sup>1,2,3,\*</sup>, James Jianqiao Yu<sup>4</sup>, Xiangyu Zhao<sup>2</sup>, Xuetao Wei<sup>1</sup>, Yuxuan Liang<sup>3</sup>

<sup>1</sup>Southern University of Science and Technology

<sup>2</sup>City University of Hong Kong

<sup>3</sup>The Hong Kong University of Science and Technology (Guangzhou)

<sup>4</sup>University of York

zhuys2019@mail.sustech.edu.cn, james.yu@york.ac.uk, xianzhao@cityu.edu.hk

weixt@sustech.edu.cn, yuxliang@outlook.com

## ABSTRACT

Human trajectory modeling is essential for deciphering movement patterns and supporting advanced applications across various domains. However, existing methods are often tailored to specific tasks and regions, resulting in limitations related to task specificity, regional dependency, and data quality sensitivity. Addressing these challenges requires a universal human trajectory foundation model capable of generalizing and scaling across diverse tasks and geographic contexts. To this end, we propose **UniTraj**, a **U**niversal human **T**rajectory foundation model that is task-adaptive, region-independent, and highly generalizable. To further enhance performance, we construct **WorldTrace**, the first large-scale, high-quality, globally distributed dataset sourced from open web platforms, encompassing 2.45 million trajectories with billions of points across 70 countries. Through multiple resampling and masking strategies designed for pre-training, UniTraj effectively overcomes geographic and task constraints, adapting to heterogeneous data quality. Extensive experiments across multiple trajectory analysis tasks and real-world datasets demonstrate that UniTraj consistently outperforms existing approaches in terms of scalability and adaptability. These results underscore the potential of UniTraj as a versatile, robust solution for a wide range of trajectory analysis applications, with WorldTrace serving as an ideal but non-exclusive foundation for training.

## 1 INTRODUCTION

Human trajectory data, which captures the movement paths of individuals or groups over time, has become increasingly significant in various domains such as transportation management [25], logistics optimization [13], and web-based services [43]. With the widespread adoption of GPS-enabled devices and the integration of positioning technologies into numerous applications, vast amounts of trajectory data are generated daily from vehicles and mobile devices connected to the Internet [18, 24, 34]. This type of data permits us an unprecedented opportunity to analyze movement patterns, traffic flow, and user mobility behaviors, supporting a range of applications from real-time traffic updates to location-based services and personalized content recommendations [3].

To effectively harness this wealth of data, robust human trajectory modeling techniques are essential to extract meaningful insights. Modeling trajectories allows us to convert raw location data into actionable information, uncovering human mobility patterns

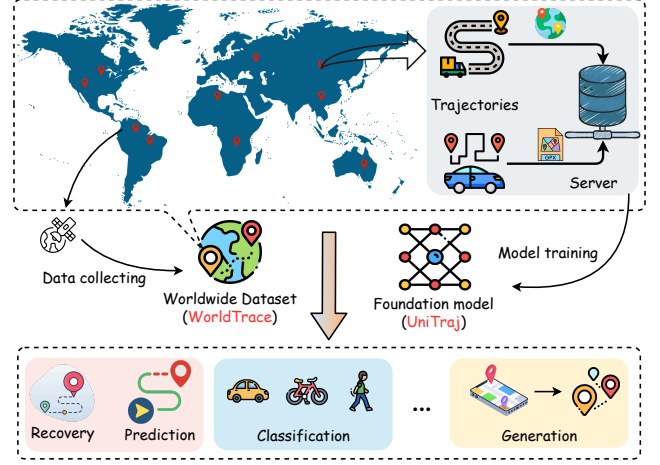


**Figure 1: Overview of this work, we propose a trajectory foundation model and also collect a worldwide trajectory dataset. The pre-trained UniTraj can be used as a backbone while adapters are trained for different regions and tasks.**

across spatial and temporal dimensions to enable advanced applications in diverse fields [2]. From a task-oriented perspective, existing methods often utilize various statistical and machine learning techniques (e.g., CNNs and RNNs) to capture detailed spatio-temporal features [20]. These models are typically optimized for specific tasks, with algorithms and architectures tailored to address distinct challenges such as trajectory prediction, anomaly detection, and activity recognition [23]. On the data side, researchers employ a wide array of trajectory datasets gathered from sources like vehicles, mobile devices, and other GPS-enabled equipment [3, 25]. These datasets vary significantly in size, geographic coverage, and quality, providing essential support for model development and evaluation. Collectively, these task-specific modeling efforts and diverse data sources have propelled advancements in human trajectory analysis, deepening our understanding of mobility behavior.

Despite these advancements, existing methods face significant limitations that impede their generalizability and practical applicability: Despite these advancements, existing methods face (i) **Task Specificity**: Current approaches are typically designed and optimized for specific tasks, lacking the flexibility to adapt across different applications without extensive modifications. This task-centric focus restricts their reusability across a range of trajectory-related

\* Work done during the internship at HKUST(GZ).

problems, including prediction, classification, and anomaly detection. (ii) **Regional Dependency**: Many models are developed and trained on data from specific geographic regions, limiting their effectiveness when applied to trajectories from diverse locations. Variations in infrastructure, traffic patterns, and behaviors across regions mean that models confined on narrow geographic data often fail to capture the diversity essential for global trajectory datasets, thus struggling to generalize to new environments. (iii) **Data Quality Sensitivity**: Real-world trajectory data is inherently heterogeneous, with variability in sampling rates, noise levels, and occasional missing data due to differences in data collection criteria and device capabilities. Existing models are typically sensitive to these inconsistencies, leading to degraded performance when faced with noisy or incomplete data. This sensitivity requires extensive data preprocessing and cleaning, which may not always be practical, reducing the robustness of these models in real-world scenarios.

What measures can be taken to overcome these limitations? Empirically, developing a task-adaptive, region-independent, and scalable foundation model for universal trajectory modeling is both an emerging necessity and a promising trend [41]. As shown in Figure 1, such a model can generalize across various tasks without requiring specialized models for each application, thereby enhancing scalability and efficiency. Additionally, a foundation model can effectively handle diverse data qualities, making it adaptable to real-world scenarios where data variability is the norm. However, constructing a universal trajectory foundation model presents two primary challenges:

- **Data preparation**: Constructing a foundation model requires the collection and integration of vast amounts of high-quality trajectory data, covering different geographic regions, sampling rates, and user behaviors. However, most existing datasets are primarily held by a limited number of companies or organizations with proprietary rights or restrictive access policies, hindering widespread usage and collaborative research. Furthermore, the labor and financial costs associated with data collection make obtaining large-scale, high-quality trajectory datasets particularly difficult. As a result, available datasets (such as GeoLife [45] and Porto [26]) are often restricted to specific regions or cities, reducing their generalizability and constraining research aimed at broader, global applications.
- **Model Design**: A universal trajectory foundation model must be equipped several capabilities that current approaches lack. First, the model should be capable of generalizing across diverse spatio-temporal contexts, enabling it to serve as a backbone that can be adapted to a wide range of tasks without extensive modifications. Second, it must maintain robust representation capabilities to handle data with varying qualities, demonstrating resilience to noise, missing values, and inconsistent sampling rates. Finally, the model should balance complexity and computational efficiency, avoiding overfitting to specific data patterns while remaining scalable for large datasets.

With these challenges in mind, we introduce WorldTrace, the first large-scale, high-quality, globally distributed trajectory dataset sourced from open platforms. Spanning 2.45 million trajectories with billions of points across 70 countries, WorldTrace overcomes the limitations of existing datasets by offering extensive geographic

coverage, diverse sampling rates, and accessible data, thereby calling widespread use and collaboration. Meanwhile, we present **UniTraj**, a **Universal human Trajectory** foundation model designed to be task-adaptive, region-independent, and resilient to varying data quality. UniTraj can serve as a versatile backbone capable of supporting diverse trajectory analysis tasks without dependence on a specific dataset, though it achieves optimal performance when trained on high-quality, diverse data like WorldTrace. In addition, our approach employs advanced pre-training techniques, including multiple resampling and masking strategies, which enable UniTraj to capture complex spatio-temporal dependencies and adapt to heterogeneous data characteristics across regions and sampling frequencies. This design promotes robust generalization across tasks and regions, offering a scalable and efficient solution for a wide range of trajectory analysis applications.

In summary, the contributions of our research are as follows:

- We construct the first large-scale, high-quality, globally distributed trajectory dataset, called WorldTrace. This dataset overcomes the limitations of existing datasets by offering accessible data for widespread use and collaboration, facilitating research with a broader global perspective, and supporting the development of universal trajectory models.
- We propose UniTraj, a universal human trajectory foundation model that leverages advanced techniques such as multiple resampling and masking strategies. UniTraj can serve as a backbone to capture complex spatio-temporal dependencies and adapts to heterogeneous data characteristics across different regions and sampling rates.
- We conduct extensive experiments across diverse trajectory analysis tasks and real-world datasets, demonstrating the scalability and adaptability of UniTraj. Additionally, we validate the unique advantages of WorldTrace, highlighting its potential as an ideal dataset for building robust and generalizable trajectory models.

## 2 PRELIMINARY

In this section, we introduce the fundamental concepts and problem statements pertinent to our work, followed by a background introduction about trajectory dataset and foundation models.

### 2.1 Problem Definition

**Definition 1 (Human Trajectory)**. Trajectory refers to the sequential record of the movement of individuals or groups through space over time. Formally, a trajectory  $\tau$  of length  $n$  is represented as a sequence of continuously sampled GPS points:  $\tau = \{p_1, p_2, \dots, p_n\}$ , where each point  $p_i = \langle \text{lng}_i, \text{lat}_i, t_i \rangle$  denotes the spatial coordinates (longitude and latitude) at timestamp  $t_i$ . In addition, the *sampling interval* between two consecutive points is defined as  $\Delta t_i = t_i - t_{i-1}$ , for  $i = 2, \dots, n$ . Note that the sampling intervals within or between trajectory data may be consistent or inconsistent.

**Definition 2 (Trajectory Dataset)**. A trajectory dataset is a collection of multiple trajectories, each representing the movement of an object over time. Formally, a trajectory dataset is defined as:  $\mathcal{D} = \{\tau_1, \tau_2, \dots, \tau_{|\mathcal{D}|}\}$ , where  $|\mathcal{D}|$  is the total number of trajectories within the dataset.

**Problem Statement (Universal Trajectory Modeling)**. The primary objective of this study is to develop a foundation model for

universal human trajectory data that can adaptively operate across different applications and geographic regions while processing heterogeneous data sources. Formally, the problem is defined as follows: Given a set of trajectories  $\mathcal{D} = \{\tau_i\}_{i=1}^{|\mathcal{D}|}$ , where each trajectory  $\tau_i$  is as defined in Definition 1, the goal is to learn a mapping function:

$$F : \tau \mapsto \mathbf{h} \in \mathbb{R}^d, \quad (1)$$

which maps a raw trajectory  $\tau$  to a  $d$ -dimensional representation tensor  $\mathbf{h}$ . The function  $F(\cdot)$  should be capable of capturing the intrinsic spatial-temporal patterns inherent in the trajectories. These trajectory representations  $\mathbf{h}$  are intended to support various analytical tasks across different regions and applications, such as trajectory classification, prediction, and anomaly detection. The model should generalize well to unseen data and be robust to the heterogeneity present in real-world trajectory datasets.

## 2.2 Related Work

**2.2.1 Trajectory Datasets.** The availability of comprehensive trajectory datasets is fundamental for advancing research in trajectory-related analysis. Over the years, several datasets have been developed, each differing in source, geographic coverage, granularity, and data quality (Note that we only focus on GPS trajectory data, other types of disjoint point-of-interest sequences are not discussed in this paper) One of the most renowned datasets is GeoLife [44], collected over five years (from April 2007 to August 2012) by 182 users. This dataset has been instrumental in various research domains such as travel mode detection [5], location recommendation [7], and traffic flow analysis [19]. Despite its extensive application, GeoLife is limited by its coverage and participant diversity, capturing movement patterns from a relatively small population. Datasets like Porto [26], T-drive [37], and Electric Vehicle Data [32] are collected through GPS devices mounted on taxis. These datasets provide a broader picture of the activities of multiple individuals but typically offer low or uneven sampling rates, which limits detailed movement pattern analysis. As a synthetic dataset, SynMob offers a uniform sampling rate and an unlimited amount of data [46], but its quality and regions still depend on the original data. Proprietary datasets like GAIA Initiative by Didi Chuxing [9], Grab-Posisi [16], and Taxi-Shanghai have released a series of high-quality trajectory datasets [9]. But these datasets are often restricted access because of authority concerns and regulation limitations, limiting their availability for widespread research and collaboration.

In summary, while existing trajectory datasets have significantly contributed to urban mobility research, they are frequently constrained by limitations such as restricted geographic coverage, low sampling rates, limited participant diversity, accessibility issues, and data quality inconsistencies. These challenges highlight the need for alternative trajectory data sources that offer extensive coverage, high-quality data, and open accessibility. Such datasets would enhance the scope and quality of urban traffic analysis and support the development of more generalizable and robust trajectory models.

**2.2.2 Foundation Models.** In recent years, foundation models have significantly advanced the fields natural language processing (NLP) and computer vision (CV), the development of foundation

models specifically tailored for trajectory data remains largely underexplored. Trajectory data present unique challenges, such as irregular sampling intervals, spatial heterogeneity, and complex temporal dependencies, which are not fully addressed by existing time series or spatio-temporal models. In domains like NLP and CV, models such as BERT [8], GPT-3 [1], and Vision Transformers (ViT) [10] have shown that it is possible to learn powerful, generalizable representations through large-scale pretraining, enabling the models to be adapted for a variety of downstream tasks. Building upon these, researchers have begun exploring foundation models for time series and spatio-temporal data. In time series analysis, models like TST [40], TimeFM [6], and Moirai [35] employ Transformer architectures [31] to capture temporal dependencies and patterns in sequential data, facilitating applications in forecasting, anomaly detection, and classification. For spatio-temporal prediction, efforts have been made to develop models that handle data varying over both space and time, such as UniST [39] and ClimaX [27], which are traffic flow prediction and climate modeling. However, trajectory data introduces additional complexities, as models must not only capture spatio-temporal dependencies but also handle noise, missing data, and varying data quality. Although some efforts have been made towards trajectory-specific models, such as TrajGDM [4] and TrajFM [22], these models are typically task-specific or regionally focused, lacking the generalization capabilities and robustness seen in other domains. For example, while foundation models like MAE [14] and TimeFM [6] have demonstrated success in unsupervised learning for image and time series data, trajectory models require even more flexibility to transfer across regions and tasks. The existing approaches often fail to provide the backbone structure needed to serve diverse scenarios without customizing stand-alone models for each task or region.

Therefore, there is a pressing need for trajectory foundation models that can unify various trajectory-related tasks under a single, pre-trained framework, similar to how foundation models in NLP and CV offer robust and transferable representations across tasks. Such models must generalize across tasks, exhibit strong representational capabilities despite data variability, and maintain computational efficiency to prevent overfitting while scaling across different applications and regions.

## 3 WORLDTRACE DATASET CONSTRUCTION

In this section, we introduce WorldTrace, a comprehensive and globally distributed trajectory dataset that overcomes the limitations of existing datasets. We detail the data acquisition process, describe the preprocessing steps, and present key statistics and analyses. As shown in Figure 2, WorldTrace provides extensive geographic coverage, encompassing trajectory data from 70 countries and spanning diverse environments and infrastructure types. This global distribution, visualized in Figure 2(a), illustrates a dense representation in North America, East Asia, and parts of Europe, with trajectory counts exceeding  $10^7$  in the most represented regions. Figure 2(b) displays the top 10 countries by trajectory counts, with the United States, China, and Canada leading in data volume. This distribution highlights the diversity of movement patterns captured in the dataset, spanning both developed and emerging economic areas. Furthermore, Figure 2(c) shows the data density

within the contiguous United States, demonstrating high-resolution coverage along major road networks and urban centers. Together, these figures emphasize the potential of WorldTrace to be suitable for the development of region-independent and universal trajectory foundation models.

### 3.1 Data Acquisition

The raw data for WorldTrace is sourced from the shared trajectory trace platform on OpenStreetMap (OSM) [28], which has hosted over 11 million GPS trajectories contributed by users worldwide since 2004. This platform<sup>1</sup> provides a rich repository of movement data suitable for large-scale analysis. To ensure data quality and reliability, we specifically filtered for vehicle trajectory data uploaded between 2021 and 2023, focusing on tags that indicated motorized movement. By prioritizing recent and labeled data, we mitigated challenges related to variable data quality, device heterogeneity, and potential obsolescence, resulting in a more consistent and reliable dataset for developing a universal trajectory model. The raw data from OSM is provided in GPX (GPS Exchange Format) files in XML format, containing geographic coordinates (latitude and longitude), timestamps, and optional altitude information. This standardized format not only ensures uniformity in data attributes but also simplifies data parsing and preprocessing, as it captures temporal and spatial information in a structured manner. Prior to integration, we applied preprocessing to eliminate duplicate entries and anomalous data points, such as unrealistically faraway or erroneous coordinates, to enhance data consistency.

### 3.2 Data Preprocessing

During data acquisition, we encountered challenges related to inconsistent data formats and varying sampling rates. To standardize the data and ensure its suitability for modeling, we implemented a series of preprocessing steps:

- (1) **Normalization:** The raw trajectory data from the original system had a high sampling frequency of 10 Hz (10 points per second), resulting in data redundancy and increased storage requirements. To mitigate this, we resampled the trajectories to a standardized rate of one point per second. This adjustment reduced redundancy and optimized storage without sacrificing key movement details, ensuring that the temporal resolution remained sufficient to capture the dynamics of the trajectories.
- (2) **Filtering:** To improve dataset relevance and accuracy, we applied multiple filtering criteria. Trajectories with fewer than 32 points or covering distances under 100 meters were discarded, as short trips generally lack meaningful movement patterns and could introduce noise. Additionally, following standard practices [5], we removed trajectories with unrealistic speeds (e.g., over 120 km/h), which often indicate GPS errors or data anomalies. This filtering ensured that only meaningful and realistic trajectories were retained for analysis.
- (3) **Calibration:** Given that GPS signals can suffer from errors due to building obstructions, multipath effects, and receiver noise [15], we applied map-matching techniques [36] to align raw GPS points with underlying road networks. This calibration

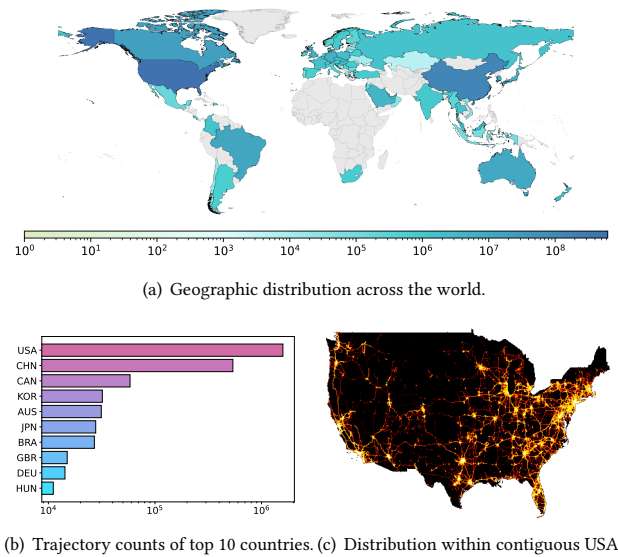


**Figure 2: The distribution details of WorldTrace dataset.**

step corrected positioning errors, improving spatial accuracy and making the trajectories more reliable for analysis.

### 3.3 Data Analysis and Statistic

After acquiring and preprocessing the raw trajectory data, we conducted an in-depth analysis to examine the characteristics and quality of the WorldTrace dataset. This analysis offers critical insights into the diversity, quality, and geographic coverage, all essential for developing a universal trajectory foundation model. Figure 2 presents a global heatmap along with the distribution of trajectories across the top 10 contributing countries within WorldTrace, highlighting a wide geographical spread that includes both developed and emerging economies. This distribution ensures various movement patterns influenced by different transportation infrastructures, cultural behaviors, and environmental conditions. We also summarize the key statistical attributes of WorldTrace in Table 1. The dataset comprises approximately 2.45 million trajectories with around 8.8 billion raw GPS points, covering 70 countries across all inhabited continents. To maintain data consistency, we normalized the sampling interval to 1 second, and the dataset spans from August 2021 to December 2023. The average trajectory duration is around 6 minutes, covering an average distance of 5.73 kilometers with an average speed of 48.0 km/h. Additionally, trajectory lengths vary significantly, from as few as 32 points to over 600 points, with an average length of approximately 358 points per trajectory. To summarize, WorldTrace provides a robust resource for training and evaluating universal trajectory models. Its extensive coverage and comprehensive statistical properties make it suitable for developing models that generalize across tasks and geographic regions, thereby addressing the limitations of existing trajectory datasets.

**Data Privacy and Copyright.** All data collection adhered strictly to privacy regulations and ethical guidelines. Trajectories were

<sup>1</sup><https://wiki.openstreetmap.org/>

**Table 1: Summary Statistics of the WorldTrace Dataset.**

Statistic	Value
Number of Trajectories	2.45 Million
Total Raw Points	8.8 Billion
Geographical Covered	70 Countries
Sampling Interval	1 sec (normalized)
Time Span	08/2021 – 12/2023
Avg. Duration	6 min
Avg. Distance	5.73 km
Avg. Speed	48.0 km/h

anonymized, and any personally identifiable information was excluded to protect user privacy. In addition, all raw data follows the Open Data Commons Open Database License (ODbL) license from OSM: <http://opendatacommons.org/licenses/odbl/1.0/>. We will share derived datasets under the same license terms to respect the data use policies of the community. Currently, we provide a data sample for reference <sup>2</sup>.

## 4 UNIVERSAL TRAJECTORY MODELING

As illustrated in Figure 3, UniTraj consists of three main components: trajectory handling and model structure, and downstream task adaptation. The trajectory handling module includes resampling and masking strategies designed to manage varying sampling intervals and enhance the model’s adaptability to different data qualities. The model structure employs a general encoder-decoder structure with tokenization and positional embedding to capture spatio-temporal dependencies. Finally, we detail the downstream task adaptation process, where pre-trained encoder of UniTraj serves as a backbone, allowing it to support multiple trajectory-related tasks with minimal additional training or fine-tuning.

### 4.1 Resampling Strategies

The sampling rate in trajectory data is crucial, as it determines the granularity of location information and the fidelity of captured motion patterns, both of which significantly impact modeling performance. However, real-world trajectories often have heterogeneous sampling rates due to differing data collection standards, device capabilities, and user behaviors. For instance, while the Porto dataset uses a 15-second sampling interval [26], the T-drive dataset averages an interval of 177 seconds [38]. Such variability introduces inconsistencies in temporal resolution, which can degrade model performance when a model trained on uniformly sampled data is applied to datasets with different sampling characteristics. This variability highlights the need for diverse temporal resolutions during training to enhance the generalization across practical scenarios. A model capable of handling different sampling rates is inherently more robust and better suited for real-world applications, where data heterogeneity is prevalent. Additionally, the diversity in trajectory lengths poses challenges in balancing data integrity and computational efficiency. Traditional uniform sampling methods struggle to handle both extremes effectively: long trajectories may

suffer from data redundancy, increased computational costs, and potential overfitting, while short trajectories risk losing critical information if undersampled, compromising the model’s ability to learn meaningful representations.

To address these challenges, we adopt two complementary resampling strategies: a dynamic trajectory resampling method and an intervals consistent resampling approach. These strategies serve two main purposes. First, they help manage data redundancy and computational load by adjusting the sampling rate according to trajectory length, ensuring efficiency. Second, they create diverse temporal intervals that improve the model’s generalization capability across datasets with varying temporal characteristics, making it better suited to handle the diverse data conditions encountered in real-world applications.

**4.1.1 Dynamic Trajectory Resampling.** We introduce a dynamic resampling strategy based on a logarithmic sampling ratio that adjusts the sampling rate according to the trajectory length. Specifically, the sampling ratio function  $R(n)$  is designed to decrease logarithmically as the trajectory length  $n$  increases:

$$R(n) = \begin{cases} R_{\min}, & n \geq n_{\max} \\ 1 - (1 - R_{\min})\phi(n), & n_{\min} < n < n_{\max} \\ 1, & n \leq n_{\min} \end{cases} \quad (2)$$

where  $R_{\min}$  is the minimum sampling ratio, and  $n_{\min}$  and  $n_{\max}$  denotes the shortest and longest length thresholds, respectively. The normalization factor  $\phi(n)$  is computed as follows:

$$\phi(n) = \frac{\ln(n - n_{\min} + 1)}{\ln(n_{\max} - n_{\min} + 1)}. \quad (3)$$

This formulation ensures that the sampling ratio decreases smoothly with increasing trajectory length, resulting in high sampling retention for shorter trajectories and a substantial reduction for longer ones. Specifically: For short trajectories ( $n \leq n_{\min}$ ): we set  $R(n) = 1$ , retaining all points to preserve detailed movement information. For long trajectories ( $n \geq n_{\max}$ ): we set  $R(n) = R_{\min}$ , significantly reducing data volume and avoiding redundancy in trajectories with many points. For intermediate trajectories ( $n_{\min} < n < n_{\max}$ ): The sampling ratio decreases logarithmically from 1 to  $R_{\min}$ , controlled by the normalization factor  $\phi(n)$ .

This dynamic adjustment offers key benefits: it controls trajectory length, reduces computational costs by eliminating redundancy, and increases dataset diversity through varied time intervals. This variability exposes the model to a wider range of sampling frequencies during training, enhancing robustness and adaptability to real-world data inconsistencies.

**4.1.2 Interval Consistent Resampling.** In addition to the dynamic resampling strategy, we employ Interval Consistent Resampling to ensure uniform temporal intervals between consecutive points within a trajectory. Specifically, this method resamples each trajectory at fixed time intervals,  $\Delta t$ , to create a standardized temporal structure across the dataset. Formally, given a trajectory  $\tau$ , we select points at intervals of  $\Delta t$ , yielding a resampled trajectory  $\tau' = p_{k_1}, \dots, p_{k_m}$ , where the indices  $k_j$  are defined as:

$$k_j = 1 + (j - 1) \cdot \Delta t, \text{ for } j = 1, 2, \dots, m, \quad (4)$$

<sup>2</sup><https://bit.ly/4fkHjBB>



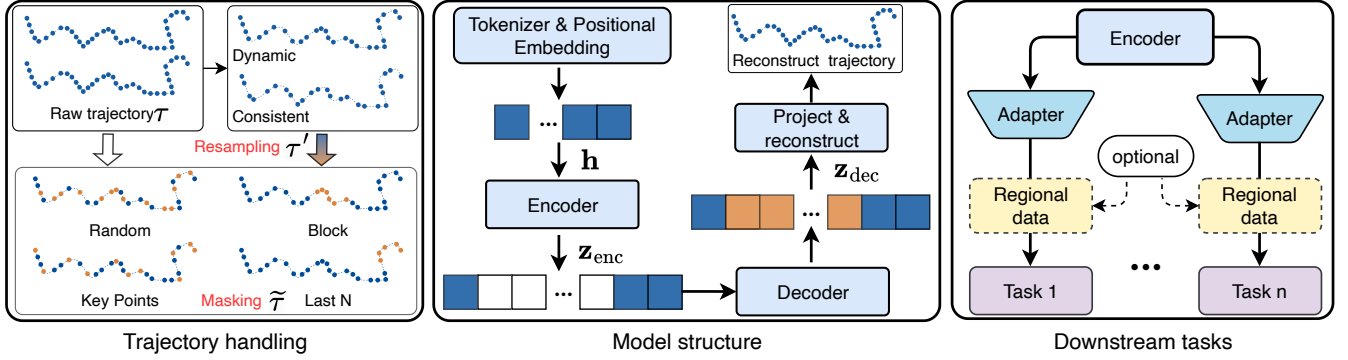


**Figure 3: Overview of the UniTraj framework, which is divided into trajectory handling and model structure, it can be employed as a backbone for downstream tasks without specific data or fine-tuning.**

with  $m$  representing the number of points in the resampled trajectory and  $\Delta t$  specifying the desired sampling interval in seconds. This approach enforces temporal uniformity, which simplifies the modeling process and enhances the model’s capacity to learn consistent temporal patterns. By mitigating issues associated with irregular or inconsistent sampling in raw data, interval consistent resampling complements the dynamic resampling strategy: while dynamic resampling adjusts sampling based on trajectory length to control data volume and introduce variability, interval consistent resampling standardizes the temporal structure across trajectories.

## 4.2 Masking Strategies

In the context of trajectory modeling, masking is essential in pre-training, as it encourages models to learn robust and generalizable representations. Inspired by self-supervised learning techniques in NLP and CV, masking entails concealing portions of the input data and requiring the model to predict the missing segments [8, 14]. This approach compels the model to capture both local and global dependencies within the data, thereby enhancing performance in downstream tasks.

Masking serves several critical functions for trajectory data. First, it acts as data augmentation, introducing variability in the input without additional data collection. Second, it strengthens model robustness by enabling it to handle incomplete or noisy trajectories issues often encountered in real-world settings due to sensor errors or communication interruptions. Finally, masking supports task-agnostic pre-training, allowing the model to learn generalized features that can later be fine-tuned for various trajectory-related tasks, such as prediction and classification. To maximize the effectiveness and compatibility of the model, we employ four distinct masking strategies, as illustrated in Figure 3. Each strategy is tailored to capture different trajectory aspects, ensuring that the model learns both global and local patterns while effectively handling diverse real-world challenges.

Formally, given a resampled trajectory  $\tau = p_1, p_2, \dots, p_n$ , we define a general masking function  $\mathcal{M}(\tau, r)$  that replaces a fraction  $r$  of the points with a mask token [MASK] at selected indices  $\mathbf{I} \subseteq \{1, 2, \dots, n\}$ ,  $r = |\mathbf{I}|/n$ . This process results in a masked trajectory:

$$\tilde{\tau} = \mathcal{M}(\tau, r) = \{p_1, \dots, [\text{MASK}]_{i \in \mathbf{I}}, \dots, p_n\}. \quad (5)$$

To comprehensively capture various patterns within the trajectory data, we employ four distinct masking strategies:

- **Random Masking:** In this strategy, we randomly select a subset of the points  $\mathbf{I}_{\text{rand}}$  to mask. By randomly masking points throughout the trajectory, the model is encouraged to learn both local and global dependencies, as the masked points are not confined to any particular position in the sequence:

$$\mathbf{I}_{\text{rand}} \sim \text{Uniform}(\{1, 2, \dots, n\}). \quad (6)$$

Random masking is effective for training the model to capture general spatio-temporal patterns across various parts of the trajectory, enhancing its robustness to missing data points.

- **Block Masking:** Block masking targets consecutive points within the trajectory, simulating scenarios where continuous segments of data may be missing. In this approach, we define blocks of a specified size  $b$  and mask all points within each block. The starting indices of the blocks are chosen randomly, creating masked indices  $\mathbf{I}_{\text{block}}$  that represent contiguous sequences of points:

$$\mathbf{I}_{\text{block}} = \{k, k+1, \dots, k+b-1\}, \text{ for some } k. \quad (7)$$

Block masking is particularly useful for teaching the model to handle longer-term dependencies, preparing it to reconstruct missing segments that may occur due to sensor failures or temporary communication losses.

- **Key Points Masking:** Key points masking focuses on significant trajectory points, such as turns or points where speed or direction changes notably. We identify these key points using the Ramer-Douglas-Peucker (RDP) algorithm [11], which simplifies a trajectory by retaining points that are farthest from the line  $\overline{p_1 p_n}$  connecting the first and last points. The indices selected for masking,  $\mathbf{I}_{\text{key}}$ , are determined by:

$$\mathbf{I}_{\text{key}} = \{p_k \mid d_{\max}(p_k, \overline{p_1 p_n}) > \epsilon\}, \quad (8)$$

where  $\epsilon$  is a predefined threshold, and the maximum distance  $d_{\max} = \max \{d(p_k, \overline{p_1 p_n}) \mid 2 \leq k \leq n-1\}$  measures deviation from this line. As summarized in Algorithm 1, the RDP algorithm iteratively identifies the point  $p_k$  that maximizes  $d_{\max} = d(p_k, \overline{p_1 p_n})$ . If  $d_{\max} > \epsilon$ , the corresponding point  $p_k$  is treated as a key point and included in the mask set  $\mathbf{I}_{\text{key}}$ . This process is recursively applied to the trajectory segments  $\tau_{\text{left}} = \{p_1, \dots, p_k\}$

**Algorithm 1** Ramer–Douglas–Peucker (RDP) Algorithm

---

```

1: function RDP( $\tau, s, e, \epsilon$ )
2:   Initialize max distance  $d_{\max} \leftarrow 0$ 
3:   Initialize index  $k \leftarrow -1$ 
4:   for  $i = s + 1$  to  $e - 1$  do
5:     Calculate the distance from  $p_i$  to  $\overline{p_s p_e}$ :  $d_i$ 
6:     if  $d_i > d_{\max}$  then
7:       Update max distance  $d_{\max} \leftarrow d_i$ 
8:       Update index  $k \leftarrow i$ 
9:     end if
10:  end for
11:  if  $d_{\max} > \epsilon$  then
12:     $\tau_{\text{left}} \leftarrow \text{RDP}(\tau, s, k, \epsilon)$ 
13:     $\tau_{\text{right}} \leftarrow \text{RDP}(\tau, k, e, \epsilon)$ 
14:    return  $\{p_k\} \cup \tau_{\text{left}} \cup \tau_{\text{right}}$ 
15:  else
16:    return  $\{p_s, p_e\}$ 
17:  end if
18: end function

```

---

and  $\tau_{\text{right}} = \{p_k, \dots, p_n\}$ , isolating critical points for masking. By focusing on these pivotal points, the model is challenged to reconstruct essential trajectory segments, reinforcing its understanding of key structural patterns within trajectories.

- **Last N Masking:** This strategy masks the last  $N$  points of the trajectory, simulating scenarios where future points are unavailable and must be inferred from observed data. The masked indices,  $I_{\text{last}}$ , comprise the last  $N$  points of the trajectory:

$$I_{\text{last}} = \{n - N + 1, n - N + 2, \dots, n\}. \quad (9)$$

This method is particularly useful for tasks such as trajectory prediction, where the model needs to predict future points based on the past observed data.

By using these four masking strategies, we can train the model to effectively predict missing parts of the trajectory while learning spatio-temporal dependencies. Each strategy introduces unique challenges, forcing the model to generalize different types of missing data scenarios, enhancing its robustness for downstream tasks.

### 4.3 Model Structure

We adopt a flexible encoder-decoder architecture for UniTraj, designed to capture both local and global trajectory patterns. This structure enables effective reconstruction and prediction of trajectories, making UniTraj adaptable to trajectory-based applications.

**4.3.1 Trajectory Tokenizer.** Effective trajectory modeling requires transforming raw spatial and temporal data into structured embeddings that capture both spatial relationships and temporal dynamics. Tokenizing trajectory data presents unique challenges due to varying trajectory lengths, the heterogeneous nature of spatial and temporal components, and the need to capture dynamic dependencies across time. To address these challenges, our trajectory tokenizer method converts spatial coordinates and timestamps into embeddings that retain individual significance and encode spatio-temporal relationships.

We use a two-part tokenizer that separately embeds spatial and temporal components and then combines them into a unified representation. For the spatial component, we normalize the trajectory to the origin by subtracting the starting point,  $(x_i, y_i) = (\text{lng}_i - \text{lng}_1, \text{lat}_i - \text{lat}_1)$ , allowing the model to focus on relative movement patterns rather than absolute locations. Each normalized spatial coordinate is transformed into a  $d$ -dimensional space using a 1D convolutional or linear layer, resulting in the spatial embedding  $\mathbf{h}_i^s = \text{Conv1D}(x_i, y_i) \in \mathbb{R}^d$ . For the temporal component, we compute the time interval between consecutive points  $\Delta t_i$  (with  $\Delta t_1 = 0$ ), embedding it into the same  $d$ -dimensional space via a linear layer, producing the temporal embedding  $\mathbf{h}_i^t = \text{Linear}(\Delta t_i) \in \mathbb{R}^d$ . We then combine the spatial and temporal embeddings by summation, yielding a unified point embedding  $\mathbf{h}_i = \mathbf{h}_i^s + \mathbf{h}_i^t \in \mathbb{R}^d$ . This final embedding effectively captures both spatial and temporal dependencies, creating a comprehensive representation for each trajectory point that is fed into the model.

**4.3.2 Positional Embedding.** In addition to encoding the spatial and temporal details of each trajectory point, it is essential to capture the relative positional relationships between points. These relationships enable the model to comprehend the movement sequence and the timing between points, both crucial for accurate trajectory modeling. To achieve this, we employ Rotary Position Encoding (RoPE) [30], which maintains the relative positional information between points by rotating the trajectory embedding vectors. Given the combined spatial-temporal embeddings  $\mathbf{h}_i$  for point  $i$  in the trajectory, RoPE applies a rotational transformation:

$$\text{RoPE}(\mathbf{h}_i) = \begin{pmatrix} \cos \theta_i & -\sin \theta_i \\ \sin \theta_i & \cos \theta_i \end{pmatrix} \begin{pmatrix} \mathbf{h}_i^{(1)} \\ \mathbf{h}_i^{(2)} \end{pmatrix}, \quad (10)$$

where  $\mathbf{h}_i^{(1)}$  and  $\mathbf{h}_i^{(2)}$  are the first and second halves of the embedding  $\mathbf{h}_i$ , and  $\theta_i$  is a rotation angle that varies proportionally with the position index  $i$ . Specifically,  $\theta_i$  is calculated as  $\theta_i = \frac{i}{10000^{2k/d}}$ , where  $k$  is the index of the embedding dimension, and  $d$  is the total dimension of the embedding.

The main advantage of RoPE is its ability to preserve relative positional information through rotational symmetry. This ensures that the relative distance and directional relationships between points are maintained, enabling the model to capture both local patterns (e.g., short-term movements) and global patterns (e.g., long-range directionality) within a trajectory. By encoding these relative positions, RoPE strengthens the model's capacity to understand movement dynamics across varying scales.

**4.3.3 Encoder-Decoder Architecture.** The UniTraj employs an encoder-decoder architecture inspired by [14], tailored for trajectory data. Both the encoder and decoder are built using stacks of Transformer blocks [31], which utilize RoPE-powered self-attention mechanisms to capture dependencies within trajectory embeddings. This architecture leverages the encoder to learn rich trajectory representations from visible points and the decoder to reconstruct masked points.

**Encoder.** The encoder processes the visible points in a trajectory, which are the unmasked points from the input sequence. The

main task of the encoder is to learn a compressed, latent representation of these visible points, capturing both spatial and temporal dependencies within the trajectory. Given a masked trajectory  $\tilde{\tau} = \{p_1, \dots, [\text{MASK}]_{i \in \mathbf{I}}, \dots, p_n\}$ , we first obtain the embedding representation of its unmasked position  $\mathbf{h} = \{\mathbf{h}_1, \mathbf{h}_2, \dots, \mathbf{h}_m\}$  ( $m \leq n$  and  $\{\mathbf{h}_i \mid i \notin \mathbf{I}\}$ ) through the trajectory tokenizer and positional encoding steps. The encoder, denoted as  $E_\theta$ , processes only the visible embeddings to produce latent representations:  $\mathbf{z}_{\text{enc}} = E_\theta(\mathbf{h})$ .

**Decoder.** The decoder reconstructs the masked trajectory points based on the latent embeddings produced by the encoder. It takes the visible embeddings along with mask tokens for the missing points, reconstructing the missing points of the trajectory. Mask tokens  $[\text{MASK}]$  are initialized as shared learnable vectors that represent masked positions. We then create the full sequence for the decoder input by merging the encoded visible embeddings with the mask tokens, aligning them to the original trajectory sequence:

$$\mathbf{z}_{\text{dec}} = \text{Reorder} \left( \left\{ \begin{array}{ll} \mathbf{z}_i = \mathbf{z}_{\text{enc},j} & \text{if } i = \text{Index}(j), i \notin \mathbf{I} \\ [\text{MASK}] & \text{if } i \in \mathbf{I} \end{array} \right\} \right), \quad (11)$$

where  $\mathbf{z}_{\text{enc},j}$  is the  $j$ -th encoder output corresponding to the  $i$ -th original position, with  $\text{Index}(j)$  mapping each visible token back to its original index. The  $\text{Reorder}(\cdot)$  function reorders tokens to their original sequence order. The decoder,  $D_\phi$ , then processes the reordered sequence to predict and reconstruct the trajectory across all positions with a linear projector:  $\hat{\tau} = \text{Linear}(D_\phi(\mathbf{z}_{\text{dec}}))$ .

#### 4.4 Training and Representing Extraction

**Training Objective.** The model is trained using a reconstruction objective, aiming to minimize the discrepancy between the predicted points and the original points  $\tau_i$  at the masked positions. The loss function is defined as follows:

$$\mathcal{L} = \frac{1}{|\mathbf{I}|} \sum_{i \in \mathbf{I}} \|f_{\theta, \phi}(\tilde{\tau})_i - \tau_i\|^2, \quad (12)$$

where  $f_{\theta, \phi}(\tilde{\tau})$  represents the encoder-decoder output, and  $i$  denotes the predicted coordinates with position. Optimizing this objective function enables the model to infer missing trajectory segments based on the observed data, allowing it to learn robust spatial-temporal dependencies essential for trajectory modeling.

**Representation Extraction.** For inference and downstream task applications, we leverage only the encoder to extract trajectory representations as follows:

$$\mathbf{z} = E_\theta(\{\mathbf{h}_i \mid i = 1, \dots, m\}). \quad (13)$$

The encoder outputs, represented by  $\mathbf{z}$ , serve as rich trajectory embeddings, which can be directly utilized for various tasks. For tasks requiring fixed-dimensional representations, a pooling operation or token selection can be applied to the sequence of encoder outputs, providing compact and informative representations tailored for downstream applications.

## 5 EXPERIMENTS

In this section, we comprehensively evaluate the performance of our proposed UniTraj across six real-world trajectory datasets, focusing on three key dimensions. We first outline the experimental setup, detailing the evaluation dimensions, datasets, and implement details. Following this, we present results and analysis for each of

the four downstream tasks, demonstrating UniTraj’s generalization ability, adaptability, and robustness across diverse trajectory analysis scenarios.

### 5.1 Experimental Setups

**5.1.1 Evaluation Dimensions.** Our experimental analysis spans three key evaluation dimensions to comprehensively assess the capabilities of UniTraj and the WorldTrace dataset. First, the **Task Applicability Analysis** examines UniTraj’s adaptability and generalizability across various trajectory-related tasks, including recovery, prediction, classification, and generation. This evaluation reveals robustness of UniTraj as a backbone architecture capable of supporting diverse geographic contexts and trajectory-based applications in real-world settings. Second, the **Dataset Study** investigates the efficacy of training on our proposed WorldTrace dataset compared to other real-world datasets. This analysis demonstrates that WorldTrace provides superior model performance, underscoring its potential as a foundational dataset for developing universal trajectory foundation models. Finally, the **Model Study** delves into the impact of architectural components, parameters, and design choices on overall performance and scalability, helping identify optimal configurations for processing large-scale trajectory data efficiently.

**5.1.2 Datasets.** We evaluate the performance of the proposed model using six diverse real-world trajectory datasets. Each dataset represents different data collection scenarios, quality levels, motion patterns, and geographic regions, providing a comprehensive test of the capabilities of UniTraj.

- **WorldTrace:** WorldTrace is our proposed large-scale, globally distributed dataset, which we describe in detail in Section 3. From the original dataset, we curated a high-quality subset of 1.1 million trajectories, which have been filtered to remove long stops and loops. Of this subset, 1 million trajectories are designated for model training combined with resampling or masking strategies, with the remaining 100,000 reserved for testing without any operation. To ensure consistency and enable independent **zero-shot evaluations**, the testing dataset is normalized to a sampling interval of 3 seconds per point.
- **Chengdu** [9]: The Chengdu dataset comprises over one million urban mobility trajectories collected from taxis operating in Chengdu, China, reflecting daily commuting and transportation patterns in a densely urbanized area. It features dense, high-frequency (3-second for most trajectories) sampling points that provide detailed insights into active urban environments.
- **Xi’an** [9]: Similar to Chengdu, the Xi’an dataset includes millions of taxi trajectories gathered in Xi’an, China, focusing on movement patterns within another densely populated Chinese city. The data, collected during November 2016, captures the traffic dynamics and urban mobility behaviors specific to this region.
- **GeoLife** [45]: The GeoLife dataset is a widely used trajectory dataset collected over three years by 182 users, primarily in Beijing, China. It is mainly distinguished by a wide variety of travel modes, including walking, cycling and driving. With this data, we can study the trajectory movement patterns and behavioral habits of different travel modes. Besides, this dataset suffers from



**Table 2: Performance comparison of UniTraj with trajectory recovery tasks. The results are reported in MAE and RMSE with meters. Bold denotes the best results and underline denotes the second-best results.**

Methods	WorldTrace		Chengdu		Xi'an		GeoLife		Grab-Posisi		Porto	
	MAE	RMSE	MAE	RMSE	MAE	RMSE	MAE	RMSE	MAE	RMSE	MAE	RMSE
Linear	427.68	516.15	205.74	258.52	176.49	220.87	196.85	249.76	507.41	617.28	396.61	482.39
DHTR	220.35	302.47	75.19	98.68	62.85	83.43	80.04	168.25	351.20	415.16	194.37	232.59
Transformer	130.82	147.62	55.23	62.85	45.85	51.96	94.68	113.77	136.58	163.29	104.36	126.96
DeepMove	51.16	62.29	29.32	39.02	27.31	35.67	86.38	107.78	126.93	168.07	136.66	174.96
TrajBERT	58.13	70.14	26.48	33.83	19.45	25.13	<u>34.53</u>	<u>43.24</u>	112.68	136.24	78.77	99.23
TrajFM	47.64	58.92	19.10	25.09	18.86	24.13	59.34	64.24	<u>107.64</u>	<u>130.69</u>	<u>71.15</u>	<u>92.96</u>
UniTraj (zero-shot)	<u>10.22</u>	<u>13.56</u>	<u>11.98</u>	<u>20.94</u>	8.93	<u>13.83</u>	37.21	63.89	114.07	167.01	78.28	100.14
Improvement(%)	$\uparrow 78.55$	$\uparrow 76.99$	$\uparrow 37.28$	$\uparrow 16.54$	$\uparrow 52.65$	$\uparrow 42.69$	$\downarrow 7.76$	$\downarrow 47.46$	$\downarrow 5.97$	$\downarrow 27.79$	$\downarrow 10.02$	$\downarrow 7.72$
UniTraj (fine-tune)	<b>6.94</b>	<b>9.67</b>	<b>6.92</b>	<b>10.41</b>	<b>6.50</b>	<b>9.93</b>	<b>23.23</b>	<b>34.70</b>	<b>48.95</b>	<b>69.23</b>	<b>60.18</b>	<b>79.76</b>
Improvement(%)	$\uparrow 85.43$	$\uparrow 83.59$	$\uparrow 63.77$	$\uparrow 58.51$	$\uparrow 65.54$	$\uparrow 58.85$	$\uparrow 32.73$	$\uparrow 19.75$	$\uparrow 54.52$	$\uparrow 47.03$	$\uparrow 15.42$	$\uparrow 14.20$

irregular and often long sampling intervals, which limit its granularity and quality for trajectory analysis.

- **Grab-Posisi** [16]: Sourced from Southeast Asia, this dataset contains 84,000 ride-hailing trajectories, predominantly from the Grab service in cities such as Jakarta and Singapore. The variable sampling intervals across these trajectories provide insights into urban mobility patterns unique to Southeast Asian metropolises.
- **Porto** [26]: The Porto dataset consists of taxi trajectories collected in Porto, Portugal, capturing trips between different areas of the city. Although it provides valuable insight into taxi mobility within the city, the dataset has a relatively low sampling frequency, with long intervals (15 seconds) between data points.

**5.1.3 Implement Details.** Our model, UniTraj, follows an encoder-decoder architecture, with the encoder comprising 8 rotary positional embedding (RoPE) empowered encoder blocks and the decoder consisting of 4 blocks. The model has approximately 2.38 million parameters, allowing it to balance complexity and computational efficiency. We set the embedding dimension to 128 and employ RoPE to capture spatial and temporal relationships effectively. During training, we use the Adam optimizer and mean square error with an initial learning rate of  $1 \times 10^{-3}$  with learning rate scheduler. We will discuss the impact of these parameter settings in detail in Section 5.4. The model is trained for 200 epochs with a batch size of 1024, and early stopping is applied based on validation performance. All experiments were conducted using PyTorch, where the foundation model is trained on NVIDIA A100/L40s 40GB GPUs and the baseline experiments are performed on RTX 2080 Ti.

## 5.2 Task Applicability Analysis

**5.2.1 Trajectory Recovery.** The objective of the trajectory recovery task is to evaluate the representation learning capability of the model by reconstructing incomplete trajectories with partially missing points. This task holds real-world significance, as trajectory data often suffers from missing points due to irregular sampling rates or sensor issues. Effective trajectory recovery showcases the ability to capture underlying spatio-temporal dependencies, enhancing robustness across varied data scenarios. In this

experiment, we randomly mask 50% of trajectory points and test the recovery performance. We evaluate UniTraj in both zero-shot (trained solely on WorldTrace) and fine-tuned settings (trained on WorldTrace and then fine-tuned on each respective dataset), aiming to understand its adaptability with and without task-specific training. Additionally, we compare UniTraj against a diverse range of baselines, including traditional deep learning models (Linear, DHTR [33], Transformer [31], and DeepMove [12]) and pre-trained models (TrijBERT [29] and TrijFM [22]). Performance metrics include Mean Absolute Error (MAE) and Root Mean Squared Error (RMSE) with meters, computed based on geographic distance.

Table 2 summarizes the recovery performance for each method across various datasets. The results show a clear trend towards generalizability, clearly highlighting the superior understanding of trajectories in different geographic and data quality scenarios by UniTraj. In the zero-shot configuration, UniTraj yields significantly lower MAE and RMSE values than traditional methods, underscoring its capacity to generalize across diverse datasets without additional fine-tuning. This indicates that UniTraj effectively captures essential spatio-temporal patterns that transfer well across diverse data sources, including datasets with different travel modes such as GeoLife and Grab-Posisi. With fine-tuning, UniTraj further improves, attaining the lowest MAE and RMSE scores across all datasets. For example, on the Xi'an dataset, UniTraj (fine-tune) reaches an MAE of 6.50, outperforming TrijFM (18.86) and DeepMove (27.31). This indicates that fine-tuning enables UniTraj to effectively adapt to the unique characteristics of each dataset, allowing for fine-grained trajectory recovery. On the GeoLife dataset, UniTraj achieves an MAE of 23.23 with fine-tuning, nearly halving TrijFM's error, which underscores its capacity to handle complex travel patterns and lower-quality data, as further evidenced in the Grab-Posisi and Porto datasets.

Overall, these findings validate the effectiveness of WorldTrace as a foundational training dataset, with UniTraj demonstrating consistent, superior performance across a range of trajectory recovery tasks and data conditions. The considerable performance gains with fine-tuning reinforce the adaptability and robustness of

**Table 3: Performance comparison of UniTraj with trajectory prediction tasks.**

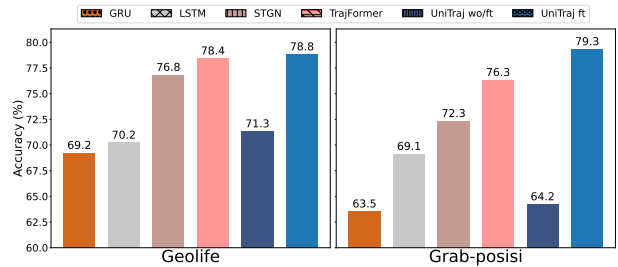
Methods	WorldTrace		Chengdu		GeoLife	
	MAE	RMSE	MAE	RMSE	MAE	RMSE
Linear	153.12	159.65	156.85	164.58	189.02	201.34
DHTR	146.48	151.63	123.47	129.73	180.32	187.59
Transformer	114.25	117.07	67.38	70.86	165.02	170.84
DeepMove	55.69	58.67	36.31	39.10	116.46	123.20
TrajBERT	80.57	86.36	64.73	68.92	113.68	121.18
TrajFM	75.45	81.32	77.82	80.48	121.94	128.16
UniTraj (zero-shot)	<u>49.85</u>	<u>55.02</u>	42.75	45.93	<u>108.35</u>	133.60
Improvement(%)	$\uparrow 10.49$	$\uparrow 6.22$	$\downarrow 17.74$	$\downarrow 17.46$	$\uparrow 4.69$	$\downarrow 10.25$
UniTraj (fine-tune)	<b>30.10</b>	<b>34.46</b>	<b>28.78</b>	<b>32.44</b>	<b>90.97</b>	<b>102.88</b>
Improvement(%)	$\uparrow 45.95$	$\uparrow 41.27$	$\uparrow 20.74$	$\uparrow 17.03$	$\uparrow 19.98$	$\uparrow 15.10$

UniTraj, making it an ideal choice for versatile trajectory-related applications.

**5.2.2 Trajectory Prediction.** The trajectory prediction task assesses the model’s capability to predict future trajectory points based on historical movement data, which is essential for applications such as navigation and traffic management. Accurate predictions indicate that the model effectively captures overall travel behavior and can infer underlying movement trends. Following the setup in prior work [22], we predict the location of five future points. The baseline settings and evaluation metrics are consistent with those used for the trajectory recovery task, and experiments were conducted on WorldTrace, Chengdu, and GeoLife datasets.

Table 3 presents the prediction performance of each baseline across the three datasets. The results show a clear advantage in the generalization and adaptability of UniTraj compared to existing methods. In the zero-shot setting, UniTraj achieves substantially lower MAE and RMSE values across all datasets, demonstrating robust performance without dataset-specific training. Fine-tuning further improves its accuracy, resulting in the lowest MAE and RMSE scores across all datasets. For instance, on the Chengdu dataset, UniTraj (fine-tune) achieves an MAE of 28.78 and an RMSE of 32.44, significantly outperforming TrajFM (77.82 MAE, 80.48 RMSE) and DeepMove (36.31 MAE, 39.10 RMSE). This improvement indicates that fine-tuning enables UniTraj to adapt effectively to the specific travel patterns within each dataset, enhancing its predictive accuracy. These results affirm UniTraj’s effectiveness in trajectory prediction tasks, demonstrating that it not only generalizes well across datasets but also benefits from fine-tuning, making it a highly adaptable model for real-world applications that require accurate trajectory predictions.

**5.2.3 Trajectory Classification.** In the trajectory classification task, we focus on the ability of UniTraj for trajectory patterns identification. Specifically, we leverage the encoder of UniTraj as a backbone and add a classifier head to distinguish various trajectory patterns. We conduct experiments on two datasets, GeoLife and Grab-Posisi, comparing UniTraj in two settings: without fine-tuning (wo/ft), where only the classifier head is trained, and with fine-tuning (ft), where the entire model is updated. For baselines, we following prior literature [21] use representative classification

**Figure 4: Performance comparison of trajectory classification task with GeoLife and Grab-posisi dataset.**

models including GRU, LSTM, STGN [42], and TrajFormer [21]. Performance is reported by classification accuracy.

As shown in Figure 4, UniTraj demonstrates strong classification performance across both datasets. On the GeoLife dataset, UniTraj achieves an accuracy of 78.8% when fine-tuned, outperforming all baseline models. Even without fine-tuning, UniTraj achieves 71.3% accuracy, indicating that its pre-trained encoder captures robust and generalizable representations. Regarding the Grab-Posisi dataset, where trajectories from motorcycles and cars are more similar in nature, UniTraj achieves an accuracy of 64.2% in the no-fine-tuning setting, still performing competitively compared to baselines trained from scratch. When fine-tuned, UniTraj reaches 79.3% accuracy, further improving its performance. These results highlight UniTraj’s effectiveness as a feature extractor for trajectory classification tasks. Its robust pre-trained representations offer a strong foundation for classification, and fine-tuning further enhances accuracy, particularly in datasets with complex or similar motion patterns.

**5.2.4 Trajectory Generation.** The trajectory generation task is designed to examine the ability of UniTraj to capture and conclude the inherent topological structure of trajectory data. In real-world applications, generating realistic trajectories is essential for tasks like urban planning, simulating movement patterns, and creating synthetic data for privacy-preserving analytics. This task thus serves to validate UniTraj’s capacity to understand structural relationships within trajectory data and generate realistic, contextually accurate paths. Following the approach in prior work [47], we assess trajectory generation using sequences of road segments that represent trajectories without explicit temporal attributes, allowing UniTraj to focus solely on topological structure. We use ControlTraj as a downstream task for trajectory generation, where we replace the road segment extraction component of the ControlTraj with UniTraj to test the effectiveness of the embedded representation. The evaluation includes *density error* metrics [47] and heatmap visualizations to measure the accuracy and realism of generated trajectories. Additionally, we assess the transferability with a cross-city experiment, training on the Chengdu dataset and testing on the Xi’an dataset, to evaluate its adaptability to new geographic contexts.

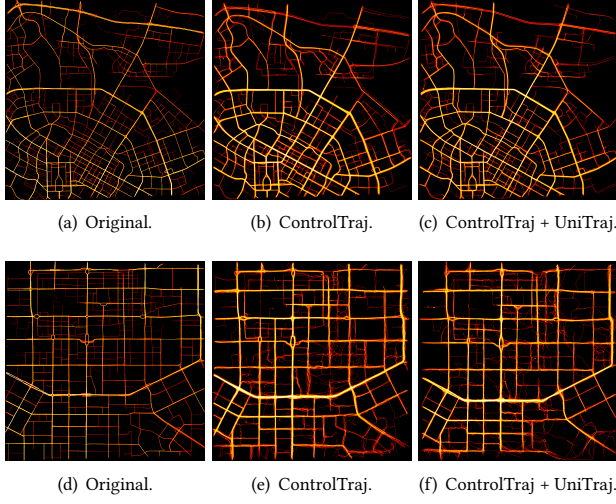


**Figure 5: Performance comparison of trajectory generation task with Chengdu dataset (first row), and transfer to Xi'an dataset (second row).**

The results in Figure 5 demonstrate the effectiveness of integrating UniTraj with ControlTraj. Visual comparisons between (b) ControlTraj and (c) ControlTraj + UniTraj for the Chengdu dataset reveal that UniTraj integration produces trajectories that more closely resemble the original (a), exhibiting refined topological alignment and path continuity. Quantitatively, UniTraj's integration improves density error performance in both intra-city and cross-city scenarios. On the Chengdu dataset, replacing road segment extraction of ControlTraj with UniTraj reduces the density error from **0.0039** to **0.0037**. The **5.1%** error reduction highlights UniTraj's enhanced capacity to capture local spatial structures. In the cross-city transfer test, where the model trained on Chengdu is applied to Xi'an, ControlTraj records a density error of **0.0171**, whereas UniTraj achieves a lower error of **0.0152** with **11.1%** improvement. These findings suggest that UniTraj's pre-trained embeddings contribute to improved generalization across cities, capturing structural patterns that extend beyond the training region. In summary, the above results underscore UniTraj's potential for robust and transferable trajectory generation, proving its effectiveness in both familiar and novel geographic settings.

### 5.3 Dataset Study

In this study, we investigate the impact of dataset scale and quality on UniTraj's performance, along with its generalization capability across different training sources, measured by MAE of trajectory recovery. Specifically, we conduct two sets of experiments: (1) analyzing the influence of varying training data volumes and quality within WorldTrace, where we train model by the full dataset (2.45 million trajectories) and a high-quality (obtained by removing loops, staying dense trajectories) {0.01, 0.5, 1} million trajectories subset to assess both scale and quality effects on model accuracy; and (2) evaluating UniTraj's ability to generalize across datasets by training it on different sources beyond WorldTrace. This second experiment

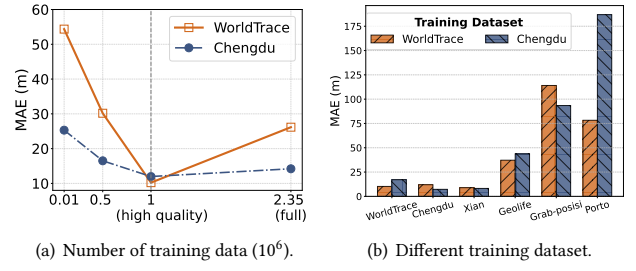


**Figure 6: The effect of amount of data volume and diversity dataset for training.**

aims to explore adaptability and effectiveness when training UniTraj on alternative datasets, thus showing its potential as a versatile trajectory foundation model.

**Effect of Dataset Scale and Quality.** Figure 6(a) shows the impact of varying amounts of WorldTrace data on the performance of UniTraj. Specifically, we observe a clear trend where the performance of UniTraj improves with increased data volume from the WorldTrace dataset, demonstrating that larger data volumes enhance the model's ability to capture diverse spatio-temporal patterns. Moreover, as we move from using a high-quality subset of 1 million trajectories to the full 2.45 million dataset, the model exhibits a slight increase in MAE. This comparison between the full dataset and the high-quality subset highlights the role of data quality; while larger datasets provide broader coverage, they also introduce more noise, and curated high-quality data contributes to more reliable and consistent learning. This suggests that both scale and quality are critical factors in achieving optimal performance, with quality being especially important when data volume is limited.

**Effect of Dataset Diversity.** In Figure 6(b), we compare the zero-shot performance of UniTraj trained on the WorldTrace and Chengdu datasets, evaluated across multiple real-world trajectory datasets. The results indicate that models trained on WorldTrace generally exhibit superior generalization across diverse datasets (e.g., GeoLife and Porto), reflecting broad geographic and contextual diversity of WorldTrace. In contrast, models trained on Chengdu perform particularly well on datasets with similar density coverage and travel modes, such as Xi'an and Grab-Posisi. However, high-quality datasets like Chengdu are typically proprietary and not publicly accessible, limiting their utility for universal applications. These findings validate UniTraj's potential as a universal trajectory foundation model, as it remains adaptable and effective even when trained on publicly available datasets like WorldTrace. Furthermore, the flexibility reinforces that while WorldTrace is optimal for foundation model training, UniTraj can effectively leverage other datasets when needed.

### 5.4 Model Study

In this section, we examine the architecture of UniTraj in detail to assess its sensitivity to parameter selection and the contribution of its core components. The first part of this analysis examines the impact of varying the number of encoder blocks and the mask ratio used during training. The purpose of this experiment is to

**Table 4: Ablation study on different resampling and masking strategies on six datasets. The results are reported in MAE and RMSE with meters. Bold denotes the best results and underline denotes the second-best results.**

Methods	WorldTrace		Chengdu		Xi'an		GeoLife		Grab-posisi		Porto	
	MAE	RMSE	MAE	RMSE	MAE	RMSE	MAE	RMSE	MAE	RMSE	MAE	RMSE
w/o Dynamic resampling	426.80	482.37	192.54	272.42	157.85	223.96	499.95	671.69	1933.28	2504.16	93.14	119.93
w/o Consistent resampling	21.30	24.76	12.98	<u>20.61</u>	9.34	13.90	69.41	115.33	<u>102.45</u>	<u>149.60</u>	1724.12	2016.61
w/o Key points masking	25.49	28.91	14.46	21.98	11.10	15.17	<u>45.94</u>	<u>72.84</u>	113.65	162.57	<b>76.51</b>	<u>101.18</u>
w/o Block masking	<b>7.79</b>	<b>10.47</b>	<b>9.22</b>	<b>15.36</b>	<b>7.16</b>	<b>11.18</b>	48.59	77.73	<b>89.34</b>	<b>128.72</b>	198.41	238.88
UniTraj	<u>10.22</u>	<u>13.56</u>	<u>11.98</u>	20.94	<u>8.93</u>	<u>13.83</u>	<b>37.21</b>	<b>63.89</b>	114.07	167.01	<u>78.28</u>	<b>100.14</b>

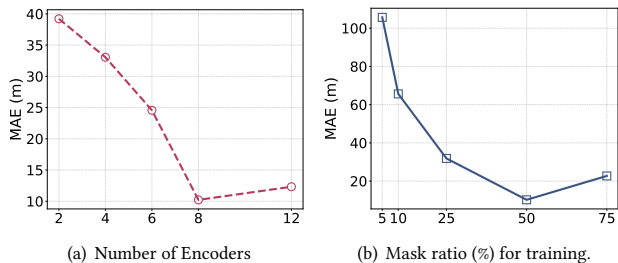


**Figure 7: The effect of different parameter settings.**

evaluate the parameter sensitivity of the model and to identify configurations that achieve the best balance of performance and efficiency. The second part of our study evaluates the individual contributions of key components, including dynamic resampling, equal time interval sampling, and masking strategies. By selectively enabling or disabling these components, we aim to understand their roles in enhancing the UniTraj’s generalizability and robustness across different datasets.

**Effect of Parameter Settings.** The parameter sensitivity analysis for UniTraj, as shown in Figure 7, provides insights into how the number of encoder blocks and the masking ratio affect model performance. In Figure 7(a), we observe that increasing the number of encoder blocks significantly enhances performance, with the MAE dropping from 40 at 2 blocks to around 10 at 8 blocks. However, adding more layers than 8 blocks does not result in additional improvement, likely due to scaling laws: as model complexity increases, larger architectures generally require more data or adjusted parameters to continue benefiting from additional capacity [17]. Figure 7(b) illustrates the impact of varying the masking ratio during training. Here, a moderate masking ratio of around 50% yields the best performance, achieving the lowest MAE. Very low masking ratios (e.g., 5%-10%) result in higher MAE, likely because they provide insufficient training signal, leading the model to overfit to observed data points. Conversely, higher masking ratios (75%) increase MAE due to excessive information loss, which limits the model’s ability to accurately reconstruct the trajectories. Thus, a 50% masking ratio strikes an effective balance, providing the model with a robust training signal while preserving adequate context for effective trajectory recovery.

**Ablation Study.** In table 4, we show the impact of each component of the model on performance. Overall, the impact of different components on different datasets are diverse, reflecting the effectiveness and limitations of each component in specific datasets and

task scenarios. This divergent performance also reflects the complexity of the model in adapting to diverse datasets. First, **Dynamic Resampling** has a significant boosting effect on the vast majority of datasets (especially the GeoLife and Grab-posisi datasets, which have lower data quality or inconsistent sampling intervals). This suggests that the component helps the model to better adapt to various data qualities and sampling frequency. This finding is further validated by removing the performance on the **Consistent Resampling** component, where the performance decrease is significant for such consistent sampling rate dataset like Porto and WorldTrace. The removal of **Key Points Masking** shows significant performance degradation on high quality datasets such as Chengdu and Xi’an, suggesting that this strategy helps the model to capture important turning points and motion patterns in such trajectories. Finally, the effect of **Block Masking** is significant on the Geolife and Porto datasets, while the performance on the other datasets is more erratic. This suggests that Block Masking is effective in handling scenarios with low sampling frequency, while it may increase the difficulty of model learning with high frequency.

In summary, the varying effects of UniTraj’s components across datasets reveal its adaptability potential for diverse tasks and scenarios. While not all components universally improve performance, their combined usage provides a balanced training strategy compatible with various datasets. In practical applications, components can be selectively enabled based on specific requirements, allowing for flexible configuration to suit particular needs. Additionally, fine-tuning the model can further enhance performance, ensuring stability and robustness across different tasks.

## 6 CONCLUSION

In this work, we presented UniTraj, a universal trajectory foundation model designed to overcome the task specificity, regional dependency, and data quality limitations of current approaches. UniTraj acts as a robust backbone that generalizes effectively across diverse tasks and regions. To support its development, we introduced WorldTrace, a high-quality global dataset with 2.45 million trajectories from 70 countries, offering broad geographic coverage, varied sampling rates, and open accessibility. Together, UniTraj and WorldTrace provide a versatile, high-performing foundation for trajectory analysis, paving the way for more adaptable and efficient models in trajectory-based research. Future work will explore further optimizations of the architecture and training strategies to enhance its effectiveness across an even broader spectrum of trajectory-related tasks.



## REFERENCES

- [1] Tom B Brown. 2020. Language models are few-shot learners. *arXiv preprint arXiv:2005.14165* (2020).
- [2] Yanchuan Chang, Egem Tanin, Gao Cong, Christian S Jensen, and Jianzhong Qi. 2023. Trajectory Similarity Measurement: An Efficiency Perspective. *arXiv preprint arXiv:2311.00960* (2023).
- [3] Wei Chen, Yuxuan Liang, Yuanshao Zhu, Yanchuan Chang, Kang Luo, Haomin Wen, Lei Li, Yanwei Yu, Qingsong Wen, Chao Chen, et al. 2024. Deep Learning for Trajectory Data Management and Mining: A Survey and Beyond. *arXiv preprint arXiv:2403.14151* (2024).
- [4] Chen Chu, Hengcai Zhang, and Feng Lu. 2023. TrajGDM: A New Trajectory Foundation Model for Simulating Human Mobility. In *Proceedings of the 31st ACM International Conference on Advances in Geographic Information Systems*. 1–2.
- [5] Sina Dabiri and Kevin Heaslip. 2018. Inferring transportation modes from GPS trajectories using a convolutional neural network. *Transportation research part C: emerging technologies* 86 (2018), 360–371.
- [6] Abhimanyu Das, Weihao Kong, Rajat Sen, and Yichen Zhou. 2023. A decoder-only foundation model for time-series forecasting. *arXiv preprint arXiv:2310.10688* (2023).
- [7] Rodrigo Augusto de Oliveira e Silva, Ge Cui, Seyyed Mohammadreza Rahimi, and Xin Wang. 2022. Personalized route recommendation through historical travel behavior analysis. *Geoinformatica* 26, 3 (2022), 505–540.
- [8] Jacob Devlin. 2018. Bert: Pre-training of deep bidirectional transformers for language understanding. *arXiv preprint arXiv:1810.04805* (2018).
- [9] Didi Chuxing. 2018. GAIA Open Datasets. <https://outreach.didichuxing.com/research/opendata/en/>
- [10] Alexey Dosovitskiy. 2020. An image is worth 16x16 words: Transformers for image recognition at scale. *arXiv preprint arXiv:2010.11929* (2020).
- [11] David H Douglas and Thomas K Peucker. 1973. Algorithms for the reduction of the number of points required to represent a digitized line or its caricature. *Cartographica: the international journal for geographic information and geovisualization* 10, 2 (1973), 112–122.
- [12] Jie Feng, Yong Li, Chao Zhang, Funing Sun, Fanchao Meng, Ang Guo, and Depeng Jin. 2018. Deepmove: Predicting human mobility with attentional recurrent networks. In *Proceedings of the 2018 world wide web conference*. 1459–1468.
- [13] Chenjuan Guo, Bin Yang, Jilin Hu, and Christian Jensen. 2018. Learning to route with sparse trajectory sets. In *2018 IEEE 34th International Conference on Data Engineering (ICDE)*. IEEE, 1073–1084.
- [14] Kaiming He, Xinlei Chen, Saining Xie, Yanghao Li, Piotr Dollár, and Ross Girshick. 2022. Masked autoencoders are scalable vision learners. In *Proceedings of the IEEE/CVF conference on computer vision and pattern recognition*. 16000–16009.
- [15] Bernhard Hofmann-Wellenhof, Herbert Lichtenegger, and Elmar Wasle. 2007. *GNSS—global navigation satellite systems: GPS, GLONASS, Galileo, and more*. Springer Science & Business Media.
- [16] Xiaocheng Huang, Yifang Yin, Simon Lim, Guanfang Wang, Bo Hu, Jagannadan Varadarajan, Shaolin Zheng, Ajay Bulusu, and Roger Zimmermann. 2019. Grab-Posisi: An Extensive Real-Life GPS Trajectory Dataset in Southeast Asia. In *Proceedings of the 3rd ACM SIGSPATIAL International Workshop on Prediction of Human Mobility*. 1–10.
- [17] Jared Kaplan, Sam McCandlish, Tom Henighan, Tom B Brown, Benjamin Chess, Rewon Child, Scott Gray, Alec Radford, Jeffrey Wu, and Dario Amodei. 2020. Scaling laws for neural language models. *arXiv preprint arXiv:2001.08361* (2020).
- [18] Hai Lan, Jiong Xie, Zhifeng Bao, Feifei Li, Wei Tian, Fang Wang, Sheng Wang, and Ailin Zhang. 2022. Vre: a versatile, robust, and economical trajectory data system. *Proceedings of the VLDB Endowment* 15, 12 (2022), 3398–3410.
- [19] Li Li, Rui Jiang, Zhengbing He, Xiqun (Michael) Chen, and Xuesong Zhou. 2020. Trajectory data-based traffic flow studies: A revisit. *Transportation Research Part C: Emerging Technologies* 114 (2020), 225–240.
- [20] Wenbin Li, Di Yao, Chang Gong, Xiaokai Chu, Quanliang Jing, Xiaolei Zhou, Yuxuan Zhang, Yunxia Fan, and Jingping Bi. 2024. Causaltad: Causal implicit generative model for debiased online trajectory anomaly detection. In *2024 IEEE 40th International Conference on Data Engineering (ICDE)*. IEEE, 4477–4490.
- [21] Yuxuan Liang, Kun Ouyang, Yiwei Wang, Xu Liu, Hongyang Chen, Junbo Zhang, Yu Zheng, and Roger Zimmermann. 2022. TrajFormer: Efficient trajectory classification with transformers. In *Proceedings of the 31st ACM International Conference on Information & Knowledge Management*. 1229–1237.
- [22] Yan Lin, Tonglong Wei, Zeyu Zhou, Haomin Wen, Jilin Hu, Shengnan Guo, Youfang Lin, and Huaiyu Wan. 2024. TrajFM: A Vehicle Trajectory Foundation Model for Region and Task Transferability. *arXiv:2408.15251* (2024).
- [23] Yan Lin, Zeyu Zhou, Yicheng Liu, Haochen Lv, Haomin Wen, Tianyi Li, Yushuai Li, Christian S Jensen, Shengnan Guo, Youfang Lin, et al. 2024. UniTE: A Survey and Unified Pipeline for Pre-training ST Trajectory Embeddings. *arXiv e-prints* (2024), arXiv–2407.
- [24] Ziqiao Liu, Hao Miao, Yan Zhao, Chenxi Liu, Kai Zheng, and Huan Li. 2024. LightTR: A Lightweight Framework for Federated Trajectory Recovery. *arXiv preprint arXiv:2405.03409* (2024).
- [25] Massimiliano Luca, Gianni Barlacchi, Bruno Lepri, and Luca Pappalardo. 2021. A survey on deep learning for human mobility. *ACM Computing Surveys (CSUR)* 55, 1 (2021), 1–44.
- [26] Wendy Kan Meghan O’Connell, moreiraMatias. 2015. ECML/PKDD 15: Taxi Trajectory Prediction (I). <https://kaggle.com/competitions/pkdd-15-predict-taxi-service-trajectory-i>
- [27] Tung Nguyen, Johannes Brandstetter, Ashish Kapoor, Jayesh K Gupta, and Aditya Grover. 2023. ClimaX: A foundation model for weather and climate. *arXiv preprint arXiv:2301.10343* (2023).
- [28] OpenStreetMap Contributors. 2024. OpenStreetMap. <https://www.openstreetmap.org>
- [29] Junjun Si, Jin Yang, Yang Xiang, Hanqiu Wang, Li Li, Rongqing Zhang, Bo Tu, and Xiangqun Chen. 2023. Trajbert: Bert-based trajectory recovery with spatial-temporal refinement for implicit sparse trajectories. *IEEE Transactions on Mobile Computing* (2023).
- [30] Jianlin Su, Murtadha Ahmed, Yu Lu, Shengfeng Pan, Wen Bo, and Yunfeng Liu. 2024. Roformer: Enhanced transformer with rotary position embedding. *Neurocomputing* 568 (2024), 127063.
- [31] Ashish Vaswani, Noam Shazeer, Niki Parmar, Jakob Uszkoreit, Llion Jones, Aidan N Gomez, Łukasz Kaiser, and Illia Polosukhin. 2017. Attention is all you need. *Advances in neural information processing systems* 30 (2017).
- [32] Guang Wang, Xiuyuan Chen, Fan Zhang, Yang Wang, and Desheng Zhang. 2019. Experience: Understanding long-term evolving patterns of shared electric vehicle networks. In *The 25th Annual international conference on mobile computing and networking*. 1–12.
- [33] Jingyuan Wang, Ning Wu, Xinxin Lu, Wayne Xin Zhao, and Kai Feng. 2019. Deep trajectory recovery with fine-grained calibration using kalman filter. *IEEE Transactions on Knowledge and Data Engineering* 33, 3 (2019), 921–934.
- [34] Yong Wang, Guoliang Li, Kaiyu Li, and Haitao Yuan. 2022. A deep generative model for trajectory modeling and utilization. *Proceedings of the VLDB Endowment* 16, 4 (2022), 973–985.
- [35] Gerald Woo, Chenghao Liu, Akshat Kumar, Caiming Xiong, Silvio Savarese, and Doyen Sahoo. 2024. Unified training of universal time series forecasting transformers. *arXiv preprint arXiv:2402.02592* (2024).
- [36] Can Yang and Gyozo Gidofalvi. 2018. Fast map matching, an algorithm integrating hidden Markov model with precomputation. *International Journal of Geographical Information Science* 32, 3 (2018), 547 – 570.
- [37] Jing Yuan, Yu Zheng, Chengyang Zhang, Wenlei Xie, Xing Xie, Guangzhong Sun, and Yan Huang. 2010. T-Drive: Driving Directions Based on Taxi Trajectories. In *Proceedings of the 18th SIGSPATIAL International Conference on Advances in Geographic Information Systems* (San Jose, California) (GIS ’10). Association for Computing Machinery, New York, NY, USA, 99–108.
- [38] Jing Yuan, Yu Zheng, Chengyang Zhang, Wenlei Xie, Xing Xie, Guangzhong Sun, and Yan Huang. 2010. T-drive: driving directions based on taxi trajectories. In *Proceedings of the 18th SIGSPATIAL International conference on advances in geographic information systems*. 99–108.
- [39] Yuan Yuan, Jingtao Ding, Jie Feng, Depeng Jin, and Yong Li. 2024. UniST: a prompt-empowered universal model for urban spatio-temporal prediction. In *Proceedings of the 30th ACM SIGKDD Conference on Knowledge Discovery and Data Mining*. 4095–4106.
- [40] George Zerveas, Srideepika Jayaraman, Dhaval Patel, Anuradha Bhamidipaty, and Carsten Eickhoff. 2021. A transformer-based framework for multivariate time series representation learning. In *Proceedings of the 27th ACM SIGKDD conference on knowledge discovery & data mining*. 2114–2124.
- [41] Weijia Zhang, Jindong Han, Zhao Xu, Hang Ni, Hao Liu, and Hui Xiong. 2024. Urban Foundation Models: A Survey. In *Proceedings of the 30th ACM SIGKDD Conference on Knowledge Discovery and Data Mining*. 6633–6643.
- [42] Pengpeng Zhao, Anjing Luo, Yanchi Liu, Jiajie Xu, Zhixu Li, Fuzhen Zhuang, Victor S Sheng, and Xiaofang Zhou. 2020. Where to go next: A spatio-temporal gated network for next poi recommendation. *IEEE Transactions on Knowledge and Data Engineering* 34, 5 (2020), 2512–2524.
- [43] Yu Zheng. 2015. Trajectory data mining: an overview. *ACM Transactions on Intelligent Systems and Technology (TIST)* 6, 3 (2015), 1–41.
- [44] Yu Zheng, Hao Fu, Xing Xie, Wei-Ying Ma, and Quannan Li. 2011. *Geolife GPS trajectory dataset - User Guide*. <https://www.microsoft.com/en-us/research/publication/geolife-gps-trajectory-dataset-user-guide/>
- [45] Yu Zheng, Lizhu Zhang, Xing Xie, and Wei-Ying Ma. 2009. Mining interesting locations and travel sequences from GPS trajectories. In *Proceedings of the 18th international conference on World wide web*. 791–800.
- [46] Yuanshao Zhu, Yongchao Ye, Ying Wu, Xiangyu Zhao, and James Jianqiao Yu. 2023. SynMob: Creating High-Fidelity Synthetic GPS Trajectory Dataset for Urban Mobility Analysis. In *Thirty-seventh Conference on Neural Information Processing Systems Datasets and Benchmarks Track*.
- [47] Yuanshao Zhu, James Jianqiao Yu, Xiangyu Zhao, Qidong Liu, Yongchao Ye, Wei Chen, Zijian Zhang, Xuetao Wei, and Yuxuan Liang. 2024. ControlTraj: Controllable trajectory generation with topology-constrained diffusion model. In *Proceedings of the 30th ACM SIGKDD Conference on Knowledge Discovery and Data Mining*. 4676–4687.